Inorganic Chemistry

Article

pubs.acs.org/IC

Selective $4e^-/4H^+$ O_2 Reduction by an Iron(tetraferrocenyl)Porphyrin Complex: From Proton Transfer Followed by Electron Transfer in Organic Solvent to Proton Coupled Electron Transfer in Aqueous Medium

Kaustuv Mittra, Sudipta Chatterjee, Subhra Samanta, and Abhishek Dey*

Department of Inorganic Chemistry, Indian Association for Cultivation of Science, Kolkata, India 700032

Supporting Information

ABSTRACT: An iron porphyrin catalyst bearing four ferrocenes and a hydrogen bonding distal pocket is found to catalyze $4e^-/4H^+$ oxygen reduction reaction (ORR) in organic solvent under homogeneous conditions in the presence of 2−3 equiv of Trifluoromethanesulphonic acid. Absorption spectroscopy, electron paramagnetic resonance (EPR), and resonance Raman data along with H_2O_2 assay indicate that one out of the four electrons necessary to reduce O_2 to H_2O is donated by the ferrous porphyrin while three are donated by the distal ferrocene residues. The same catalyst shows $4e^-/4H^+$ reduction of O_2 in an aqueous medium, under heterogeneous conditions, over a wide range of pH. Both the selectivity and the rate of ORR are found to be pH independent in an aqueous medium. The ORR proceeds via a proton transfer followed by electron transfer (PET) step in an organic medium and while a $2e^-/1H^+$ proton coupled electron transfer (PCET) step determines the electrochemical potential of ORR in an aqueous medium.

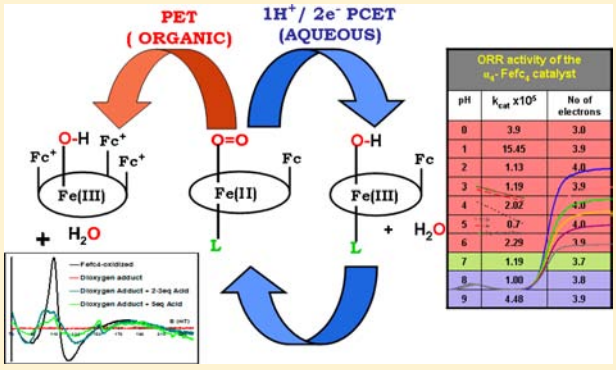

1. INTRODUCTION

The oxygen reduction reaction (ORR) is important in biological respiration as well as in H_2/O_2 fuel cell applications.[1] H_2/O_2 fuel cells oxidize hydrogen at the anode and reduce oxygen at the cathode generating an EMF of 1.23 V. A platinum catalyst is used on both cathode and anode.

$$2H_2 \rightarrow 4H^+ + 4e^- \quad \text{(Anode Reaction)}$$

$$O_2 + 4H^+ + 4e^- \rightarrow 2H_2O \quad \text{(Cathode Reaction)}$$

The ORR at the cathode is much slower than the hydrogen oxidation reaction occurring at the anode.[2] To speed up the ORR kinetics, to make practical fuel cells, an efficient ORR catalyst is required.[3,4] Platinum, even though it is the most efficient catalyst, is expensive.[2−5] Hence, extensive research over the past few decades has targeted the development of efficient non-noble metal based ORR catalysts.[6−9] This effort has led to identification of several key attributes essential for a good ORR catalyst.

It is desirable that an ORR catalyst should not only be stable but also be able to reduce oxygen efficiently over a wide range of pH. Most known metalloporphyrin based ORR electrocatalysts show optimal activity (both selectivity and rate) at a specific pH.[10−15] There are rare examples of catalysts which show comparable selectivity in acidic, neutral, and basic pHs.[16,17] Even rarer are examples of catalysts that show the same catalytic rate of ORR over a large pH range.[18] This is particularly important for applications in H_2/O_2 fuel cells. Ferrocene undergoes 1 electron oxidation to form ferrocenium and has recently been used effectively as an external electron donor in the presence of a Cu catalyst and strong acids in the four electron reduction of oxygen to water.[8] Recently an iron porphyrin complex, containing 4 electron donating ferrocene groups covalently attached to the porphyrin ring, was reported (Figure1). This complex was found to catalyze reduction of O_2 to O_2^- in an organic solvent and a selective $4e^-/4H^+$ reduction of oxygen to water at pH 7.[19] Importantly the selectivity for $4e^-/4H^+$ ORR in aqueous medium was retained under both fast and slow electron fluxes from the electrode. This was due to the availability of electron donating ferrocene groups in the molecule. The crystal structure of an analogous Zn porphyrin complex showed the presence of strong H-bonding interactions in the distal pocket facilitated by the triazole rings and mediated by water molecule. This H-bonding interaction forces axial ligands like methanol and O_2 to bind inside the sterically congested distal pocket instead of the open proximal side.[20] H-bonding residues are known to act as proton translocator for ORR catalysts. This attribute is known to aid proton coupled electron transfer (PCET) steps often invoked to be involved in ORR.[14]

Received: September 10, 2013
Published: December 4, 2013

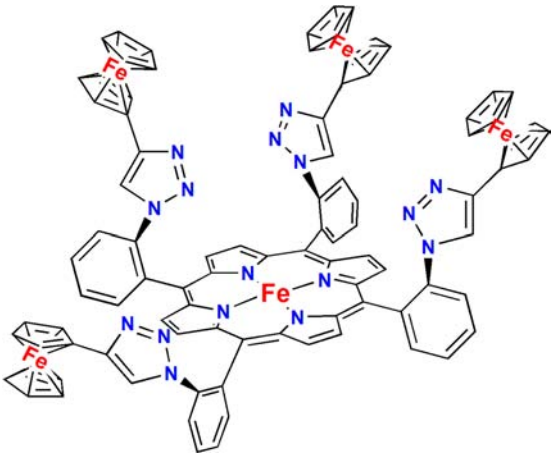

Figure 1. Schematic diagram of the α_4-FeFc4 complex.

In this paper we report that the α_4-$FeFc_4$ catalyst can, in fact, reduce O_2 to water under homogeneous conditions in an organic solvent in the presence of acid. Further this complex can catalyze ORR with almost equal efficiency in an aqueous medium, under heterogeneous conditions, over a wide range of pH (1 to 9). Not only the selectivity but also the catalytic rate of ORR is also found to be independent of pH. This is likely due to the H-bonding cavity consisting of triazoles ($pK_a \sim 1$) in the catalyst which provides efficient proton translocation into the catalytic center over the entire pH range.

2. EXPERIMENTAL DETAILS

2.1. Synthesis. The complexes are synthesized as previously reported.[19]

2.2. Materials and Methods. Sodium sulphide was purchased from Rankem, trifluoromethanesulphonic acid (triflic acid) and methanol (MeOH) were purchased from Sigma Aldrich (U.S.A.). *p*-Toluenesulfonic acid (PTSA) was purchased from Spectrochem. Unless otherwise stated all chemicals were used as purchased, and reactions were performed at room temperature. Edge Plane Graphite (EPG) discs were purchased from Pine Instruments. All the electron paramagnetic resonance (EPR) spectra were recorded on a JEOL instrument. Resonance Raman (rR) data were collected using 413.1 nm excitation from a Kr^+ ion source (Coherent Inc.) and a Trivista 555 triple spectrophotometer (gratings used in the three stages were 900, 900, and 1800 grooves/mm) fitted with an electronically cooled Pixis CCD camera (Princeton Instruments). The irradiation power was limited to 10 mW at the sample to avoid degradation. Data were collected at room temperature and 77 K for 200 s.

2.3. Electrochemical Measurements. A 50 μL portion of a dilute solution (1 mM) of the α_4-$FeFc_4$ catalyst (in $CHCl_3$) was uniformly distributed on the graphite disc. After the $CHCl_3$ had evaporated, the surface was sonicated in ethanol for 30 s and washed with triple distilled water. The linear sweep voltammetry (LSV) were recorded on electrochemical analyzer purchased from CH Instruments using CHI720 D. A Pt wire was used as a counter electrode. The measurements were made against an Ag/AgCl aqueous reference electrode with scan rates varying from 50 mV/s to 500 mV/s. 100 mM phosphate buffers were used to maintain pH from 0 to 9 (pH adjusted by adding H_3PO_4 or KOH). 100 mM KPF_6 was used as supporting electrolyte in each case.

2.4. H_2O_2 Detection and Other Experimental Details. A 1.67 mg portion of α_4-FeFc4 catalyst was dissolved in 1 mL of dry degassed tetrahydrofuran (THF) solvent so that the final strength was 1 mM. A 2.4 mg portion of Na_2S was dissolved in minimum volume of methanol and diluted with dry degassed THF to make the final volume 1 mL, so that the final strength was 10 mM. THF was rigorously degassed using the freeze−pump−thaw technique. Next, in a glovebox, 100 μL of this 1 mM $FeFc_4$ solution was added to an EPR tube (A). To three other EPR tubes (B), (C), (D), 0.5 equiv (5 μL) of Na_2S was added. It has been recently shown that in a nonpolar organic solvent Na_2S can reduce Fe^{III} porphyrin to Fe^{II} porphyrin and itself gets oxidized to elemental sulfur in the process.[21] While the sample in tube A showed a high spin Fe^{III} signal in EPR, the samples in tubes B, C, D were EPR silent indicating that all the Fe^{III} has been reduced to Fe^{II}. This was also indicated by the shift of the Soret band from 426 nm in the oxidized to 433 nm in the reduced form. Next, oxygen gas was bubbled through the solution in the EPR tubes B, C, D at −80 °C. This was followed by addition of 20−30 μL (2−3 equiv) of trifluoromethanesulphonic acid (10 mM in THF) to C and addition of about 50 μL (5 equiv) of the same acid to EPR tube D all at −80 °C. The EPR and Raman data of all tubes were recorded.

The UV experiments to monitor the oxidation of ferrocenes were done similarly except that a 0.5 mM concentration of the catalyst was used.

H_2O_2 Detection. A xylenol orange assay was used to detect H_2O_2 produced during O_2 reduction under homogeneous conditions. A 4.9 mg portion of Mohr's salt and 3.9 mg of xylenol orange were dissolved in 5 mL of 250 mM H_2SO_4 and stirred for 10 min. A 200 μL portion of this solution was taken in 1.8 mL of triple distilled water, and a calibration curve for quantitative estimation of H_2O_2 was obtained by adding 20 μL aliquots of H_2O_2 having different concentrations and recording their absorbance at 560 nm. The concentrations of H_2O_2 used were 0.05 μM, 0.1 μM, 0.5 μM, 1 μM, 2.5 μM, 5 μM, 10 μM, and 100 μM.

A 200 μL portion of the xylenol orange H_2SO_4 mixture was added to 1.8 mL of H_2O in a cuvette, and the absorbance was recorded. A 100 μL portion of 1 mM reduced $FeFc_4$ (1 mM oxidized α_4-$FeFc_4$ in THF + Na_2S (5 μL of 10 mM in THF)) in an organic solvent (THF) was exposed to dry O_2 gas at −80 °C. This solution was then extracted with 200−400 μL of H_2O. Twenty microliters of this aqueous extract was added to the cuvette containing the xylenol orange and H_2SO_4 mixture. Absorbance for this was recorded. The absorbance of the above solution (after subtracting the control) at 560 nm is fitted in the calibration curve (obtained as described above) to get the corresponding H_2O_2 concentrations.[22] This concentration is scaled accounting for dilution to get the concentration of H_2O_2 produced in the original α_4-$FeFc_4$ solution. Addition of 20 μL of the catalyst solution in THF to the xylenol orange and H_2SO_4 mixture did not result in increase of absorbance at 560 nm. The same process was repeated to acquire the data after addition of 2−3 equiv and 5 equiv trifluoromethanesulphonic acid at −80 °C to the dioxygen adducts of $FeFc_4$.

3. RESULTS

3.1. $4e^-/4H^+$ ORR in Organic Solvent (Homogeneous). The initial oxidized α_4-$FeFc_4$ in THF solvent is reduced by 0.5 equiv of Na_2S (dissolved in dry degassed methanol). The reaction of the reduced complex with O_2 in an organic solvent is followed by EPR and rR spectroscopy. EPR spectroscopy is a useful tool to determine the spin state of iron porphyrin complexes. rR can be used to determine the oxidation and spin states of iron porphyrin complexes using ν_4 and ν_2 modes of the porphyrin ring; also known as oxidation and spin state marker bands.

a. EPR. The EPR spectrum of oxidized α_4-$FeFc_4$ is shown in (Figure 2, blue). The oxidized complex exhibits a $g \sim 6$ axial EPR signal indicating that the Fe in the α_4-$FeFc_4$ complex is in a high-spin $S = 5/2$ Fe^{III} state. On reduction the complex becomes EPR silent consistent with the formation of a reduced Fe^{II} complex. Upon exposing the reduced sample to O_2 at −80 °C no new EPR signal is observed (Figure 2, red) suggesting the presence of a diamagnetic dioxygen adduct.[23] On addition of 2−3 equiv and excess (5 equiv) of trifluoromethanesulphonic acid (triflic acid) to the dioxygen adduct, a new rhombic

dx.doi.org/10.1021/ic402297f | *Inorg. Chem.* 2013, 52, 14317−14325

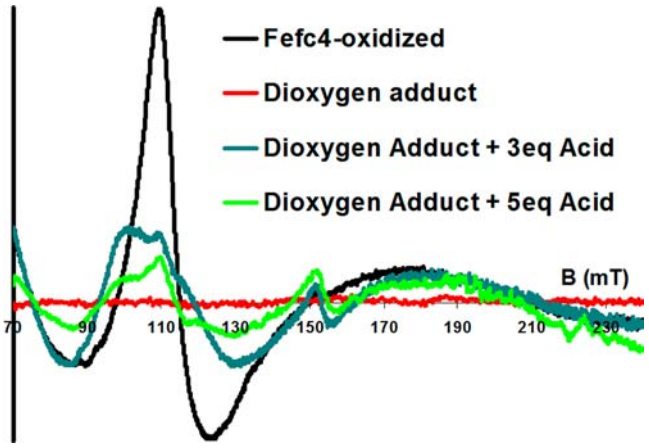

Figure 2. EPR spectra of $FeFc_4$ showing the oxidized, dioxygen adduct and the final product at room temperatue after addition of 3 equiv and excess of triflic acid at −80 °C.

signal at $g \sim 6$ (Figure1, green) is obtained indicating that the complex returns to a high spin Fe^{III} oxidation state. The rhombicity in the EPR spectra of the final product is due to the replacement of the Br^- counteranion present in the starting complex by a π anisotropic hydroxo or methoxy ligand in the final product.[20]

b. Resonance Raman. rR data of the oxidized sample shows that the oxidation and spin state marker ν_4 and the ν_2 bands are at 1361 cm^{-1} and 1552 cm^{-1}, respectively (Figure 3, black),

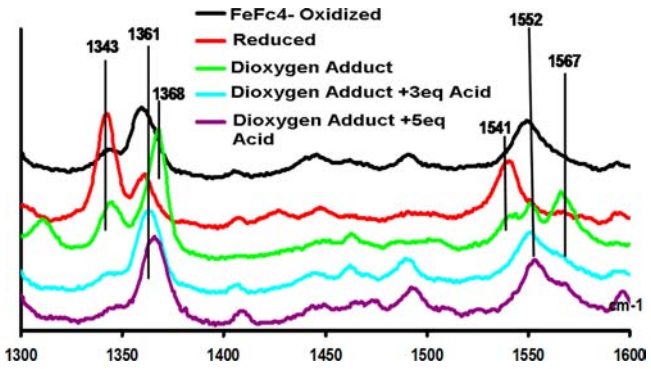

Figure 3. rR data of the as isolated α_4-$FeFc_4$ complex (black), the fully reduced α_4-$FeFc_4$ complex (red), the oxygen adduct (green, note some of the reduced complex is still present as indicated by the presence of a weak ν_4 band at 1346 cm^{-1}) and the final product (blue). 1 mM in THF, 413.1 nm excitation, 77 K, 10 mW.

which are typical of $S = 5/2$ Fe^{III} porphyrins, consistent with the EPR data (Figure 2, black).[24] Upon reduction these bands shift to 1343 cm^{-1} and 1541 cm^{-1}, indicating the formation of a high-spin $S = 2$ Fe^{II} species (Figure 3, red). The diamagnetic O_2 adduct shows a new set of bands at 1368 cm^{-1} and 1568 cm^{-1} (Figure 3, green).[24] This species is an end-on $S = 0$ $Fe^{II}-O_2$ adduct (Supporting Information, Figure S1).[23] Dioxygen adduct of a ferrous porphyrin can be described as $Fe^{II}-O_2$ or $Fe^{III}-O_2^-$. Recent X-ray absorption data and its analysis indicate that none of the limiting descriptions may be adequate.[25] Thus this species is referred to as a $Fe^{II}-O_2$ species in the rest of the paper. On addition of 2−3 equiv of triflic acid to the diamagnetic dioxygen adduct at −80 °C initially causes no change. However, warming up to about −40 °C results in shifting of the ν_4 and the ν_2 bands to 1363 cm^{-1} and 1553 cm^{-1}(Figure 3, sky blue), respectively. Addition of 5 equiv of triflic acid follows the same trend, and the bands shift to 1364 cm^{-1} and 1553 cm^{-1} (Figure 3, violet). Thus, it is clear that in both cases a high spin Fe^{III} species is formed when the diamagnetic $Fe^{II}-O_2$ adduct of the α_4-$FeFc_4$ complex is treated with triflic acid. This is consistent with the EPR data. Note that both the rR (ν_4 and ν_2 bands are different) and the EPR data (the product has more rhombic character) indicate that the starting high-spin Fe^{III} α_4-$FeFc_4$ complex is different from the final product after addition of 3 and 5 equiv of acid.[26] There is however no change in the rR data in the presence of a weaker acid, *p*-toluenesulphonic acid (PTSA, $\mathbf{pK_a = 8.5}$) compared to triflic acid ($\mathbf{pK_a = 0.3}$) or in the presence of methanol ($\mathbf{pK_a = 27.9}$) which can also act as a proton source. Even addition of 1 equiv of triflic acid does not change the EPR or rR spectra.

c. H_2O_2 Assay. Hydrolysis of the $Fe^{II}-O_2$ adduct prepared in homogeneous organic medium yielded 48 ± 3% H_2O_2 in the resultant solution, that is, the α_4-$FeFc_4$ catalyst selectively reduces O_2 to O_2^- and not H_2O in a nonpolar organic solvent (O_2^- disproportionate to H_2O_2 and O_2 yielding an overall 50% H_2O_2).[20,22] On addition of 2−3 equiv of triflic acid to the $Fe^{II}-O_2$ complex yielded only 1−5% H_2O_2. This is an interesting observation as it indicates that addition of 2−3 equiv of triflic acid to the $Fe^{II}-O_2$ adduct leads to $4e^-$ reduction of O_2 to H_2O while the lack of acid produces 50% H_2O_2. This implies that the presence of acid is necessary to drive $4e^-$ reduction of O_2, that is, the ORR catalyzed by α_4-$FeFc_4$ catalyst likely involves a proton assisted step. However 50% of H_2O_2 is detected when 1 equiv of triflic acid or a weaker acid like PTSA or when no acid is used instead, that is, the reaction is stalled at the $Fe^{II}-O_2$ stage under these conditions. Alternatively, when more than 5 equiv of triflic acid is added ~50% H_2O_2 is observed, that is, significant $2e^-/2H^+$ ORR is observed when excess acid is used, implying hydrolysis of the $Fe^{II}-O_2$ or $Fe^{III}-OOH$ intermediates (Scheme 3) to yield H_2O_2 under strongly acidic conditions.

d. Quantification of Ferrocenium Produced during O_2 Reduction. The UV spectrum (Figure 4) shows a new

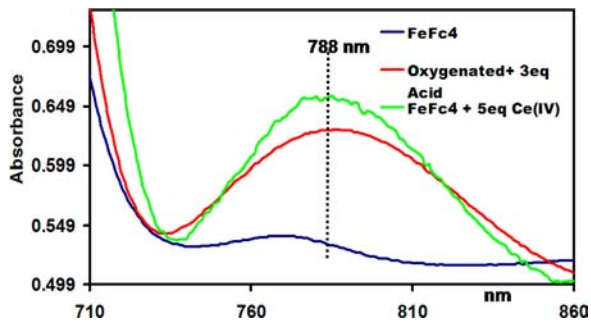

Figure 4. UV spectra in the region of 700−860 nm showing the $FeFc_4$ catalyst in its initial oxidized state (blue) and after addition of 5 equiv of CAN (green). The spectrum in red is obtained after adding 3 equiv of triflic acid to the oxygenated catalyst at 298 K.

absorbance band at 788 nm after addition of ~3 equiv of triflic acid to the oxygenated α_4-$FeFc_4$ at 298 K. Neither the oxidized nor the reduced α_4-$FeFc_4$ complex show a λ_{max} at 788 nm and thus this new band at 788 nm indicates the 1 electron oxidation of the ferrocene groups of the complex.[27−29] Thus, the ferrocene groups supply the electrons necessary for reduction of oxygen to water in organic medium, in the presence of 2−3 equiv of acid as they themselves get oxidized to ferrocenium. Further in an effort to quantify the number of

dx.doi.org/10.1021/ic402297f | *Inorg. Chem.* 2013, 52, 14317−14325

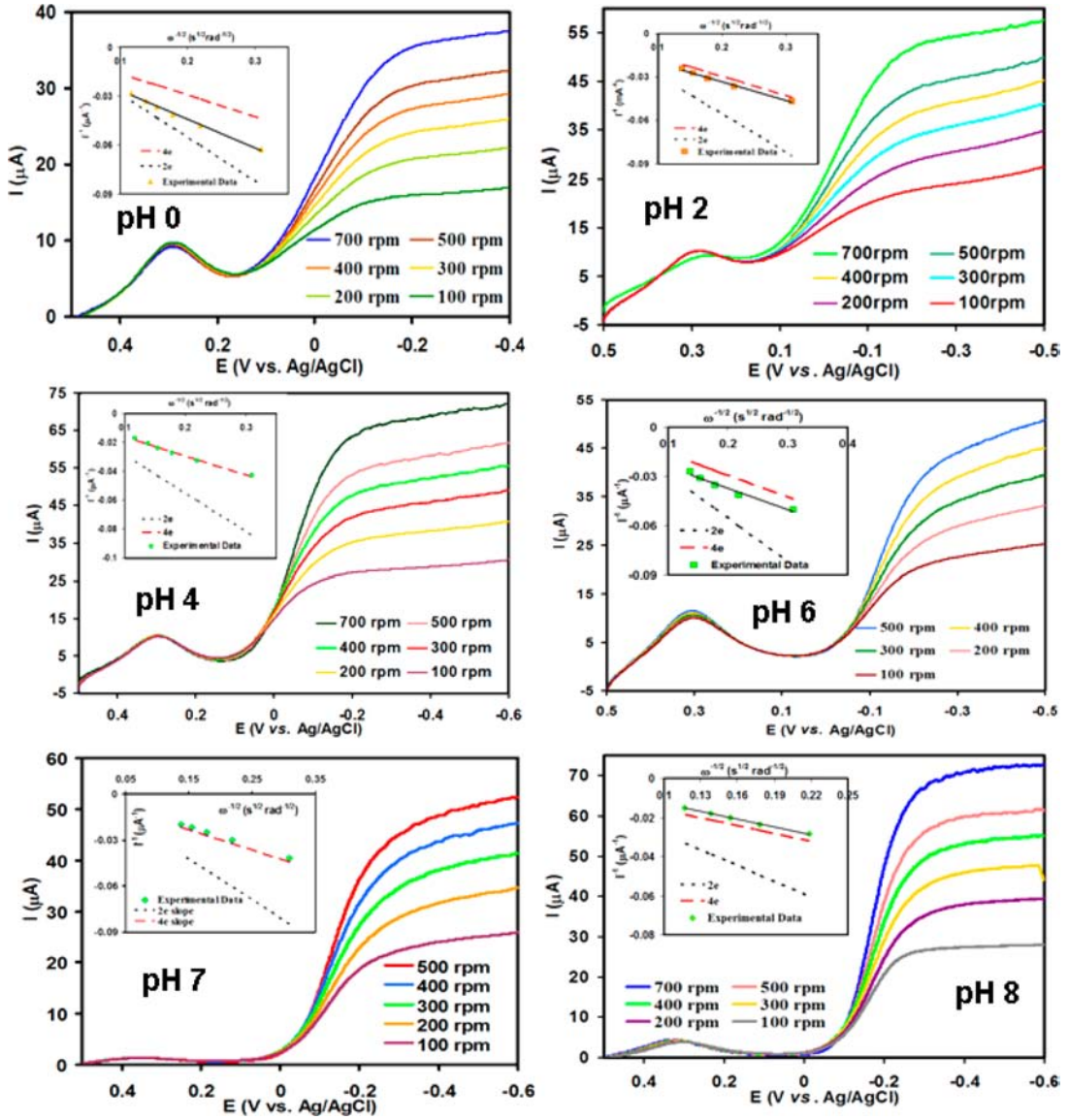

Figure 5. LSV data of α_4-$FeFc_4$ deposited on EPG surface at multiple rotations in pH 0, pH 2, pH 4, pH 6, pH 7, pH 8 phosphate buffers, using 100 mM KPF_6 as the supporting electrolyte and Pt and Ag/AgCl as counter and reference electrodes, respectively. (inset) K-L plot of the α_4- $FeFc_4$ catalyst (black bold line). The theoretical plots for 4e- and 2e- processes are indicated by dashed (red) and dotted lines (black), respectively. The RDE data for pH 1, pH 3, pH 5, pH 9 are shown in Supporting Information, Figure S2.

ferrocenes getting oxidized, a methanol solution of cerric ammonium nitrate (CAN) is added to the α_4-$FeFc_4$ solution, where the iron in the porphyrin is in the oxidized ferric state while the ferrocenes are reduced. CAN being a strong oxidizing agent (E^0 = 1.39 V vs Ag/AgCl) can oxidize the ferrocenes (E^0 = 0.73 V vs Ag/AgCl) present in the complex. Since, each α_4-$FeFc_4$ molecule contains 4 ferrocene groups, increasing equivalents of CAN is added to oxidize the ferrocenes to ferroceniums. The resultant spectrum (green) showed a peak at 788 nm indicating the oxidation of ferrocene groups. Approximately 5 equiv of CAN is required to oxidize all the ferrocene groups (Supporting Information, Figure S4). The ratio of the intensities at 788 nm for the spectrum obtained after reduction of the O_2 in presence of ~3 equiv of acid and the spectrum obtained after the oxidation of the four ferrocene groups in α_4-$FeFc_4$ indicate that only 80% of the ferrocenes present in the catalyst are oxidized to ferrocenium during the reduction of oxygen to water. Since, oxidation of three ferrocenes out of four should yield a ratio of 0.75, the observed ratio of 0.8 thus implies that only 3 electrons for the reduction of oxygen to water are derived from the ferrocenes while the fourth is supplied by Fe when it gets oxidized from +2 to +3 as is indicated by EPR and rR data in sections 3.1.a and 3.1.b, respectively.

3.2. $4e^-/4H^+$ ORR in Aqueous Medium (Heterogeneous). *a. Selectivity of O_2 Reduction.* Linear sweep voltammetry (LSV) data of this catalyst immobilized on edge plane graphite (EPG) electrodes and immersed in aqueous solution show a substrate diffusion limited catalytic O_2 reduction current below −0.1 V (Figure 5) at pH 0−pH 9 in aqueous phosphate buffer solutions. The cathodic peak at +300 mV represents the reduction of the ferrocene groups, and it serves as an internal reference to quantify the amount of catalyst on the electrode as each iron porphyrin molecule contains four ferrocene substituents. Its potential does not change with pH. The onset of the catalytic current coincides

dx.doi.org/10.1021/ic402297f | Inorg. Chem. 2013, 52, 14317−14325

with the reduction of the iron in the porphyrin from the oxidized ferric state to the reduced ferrous state. The O_2 reduction current increases with increasing rotation rates following the Koutecky–Levich equation, $I^{-1} = i_K(E)^{-1} + i_L^{-1}$, where $i_K(E)$ is the potential dependent kinetic current and i_L is the Levich current. i_L is expressed as $0.62nFA[O_2](D_{O2})^{2/3}\omega^{1/2}\nu^{-1/6}$, where n is the number of electrons transferred to the substrate, A is the macroscopic area of the disc (0.125 cm^2), $[O_2]$ is the concentration of O_2 in an air saturated buffer (0.26 mM) at 25 °C, D_{O2} is the diffusion coefficient of O_2 (1.8×10^{-5} cm^2 s^{-1}) at 25 °C, ω is the angular velocity of the disc, and ν is the kinematic viscosity of the solution (0.009 cm^2 s^{-1}) at 25 °C. The plot of I^{-1} at multiple rotation rates vs the inverse square root of the angular rotation rate ($\omega^{-1/2}$) is linear. The slopes obtained from the experimental data for the catalyst at pH 1–9 is almost identical with the theoretical slope predicted for a $4e^-$ process (Figure 5 and Supporting Information, Figure S2).[30] The data at pH 0 indicates significant $2e^-/2H^+$ reduction from O_2 to H_2O_2. The turn over number (TON) of oxygen reduction by α_4-FeFc4 catalyst at pH 7 is estimated (from the amount of charge consumed and the coverage of the catalyst) to be $>10^3$ at pH 7.

b. Variation of k_{cat} with pH. The intercept of the K-L plot can be used to obtain the kinetic current, i_k, which can be used to obtain the second order ORR rates for the catalyst ($i_k = nFA[O_2]k_{cat}\Gamma_{catalyst}$, where $\Gamma_{catalyst}$ is the catalyst concentration in moles cm^{-2}). The data (Table 1) suggests that not only does the α_4-$FeFc_4$ catalyst reduce oxygen by 4 electrons in between pH 1–9, but also has the similar catalytic k_{cat} values indicating that the efficiency of the catalyst to reduce oxygen to water does not change in this pH range. Note that the k_{cat} values are corrected for differences in loading in every experiment (Supporting Information, Table S1). Thus this is a rare example of a catalyst where both the k_{cat} and the selectivity are retained in the pH range of 1–9, that is, across a proton concentration gradient of 10^9.

Table 1. ORR Activity of the α_4- $FeFc_4$ Catalyst[a]

pH	$k_{cat} \times 10^5$ (M^{-1} s^{-1})	no. of electrons	Tafel slopes (mV/dec)
0	3.9 ± 0.5	3.0	ND
1	1.0 ± 0.1	3.9	ND
2	1.1 ± 0.2	4.0	ND
3	1.2 ± 0.3	3.9	ND
4	2.0 ± 0.6	4.0	ND
5	0.7 ± 0.3	4.0	139
6	2.3 ± 0.3	3.9	136
7	1.2 ± 0.2	3.7	140
8	1.0 ± 0.1	3.8	118
9	4.5 ± 0.5	3.9	119

[a]ND = Not determined.

4. DISCUSSION

In an aqueous medium O_2 is reduced to H_2O over a wide range of pH. It is evident that the potentials for ORR (E_{ORR}) shifts toward positive values as the pH is lowered (Figure 6). A plot of E_{ORR} with pH shows a slope of 28 mV per pH unit. A general expression of the pH dependence of a Proton Coupled Electron Transfer (PCET) pathway is $-0.059f/n(pH)$, where n is the number of electrons and f is the number of protons.[31] In this case the observed slope is consistent with $n = 2$ and $f = 1$, that is, the ORR by the α_4-$FeFc_4$ catalyst involves a two electron and $1H^+$ proton step as the potential determining step.[31,32] O_2 reduction to water is a multistep reaction and several of them can show a $2e^-/1H^+$ PCET. The protonation of the $Fe^{II}-O_2$ adduct, leading to the formation of a $Fe^{III}-O_2H$ species, followed by the cleavage of the O–O bond and simultaneous protonation of the distal oxygen of the $Fe^{III}-O_2H$ species can be expected to show a $2e/1H^+$ PCET behavior (Proposal 1, Scheme 1). A similar proposal was put forward by Nocera to explain the mechanism of ORR by binuclear-cobalt pacman porphyrin.[33] Alternatively, initial protonation of a tentative Fe^{III}–OOH species followed by a O–O bond cleavage can also be expected to show a $2e^-/1H^+$ PCET pathway (Proposal 2, Scheme 1). Another likely scenario is the reduction of the Fe^{III} to Fe^{II} followed by oxygen binding and transfer of an electron and proton to the intermediate $Fe^{II}-O_2$ species to generate a $Fe^{III}-O_2^{2-}$ species (Proposal 3, Scheme 1). Similarly a coupled H^+ and e^- transfer to a $Fe^{II}-O_2$ intermediate to generate a Fe^{III}–OOH species followed by its reduction to a Fe^{II}–OOH species can also show a $2e^-/H^+$ PCET(Proposal 4, Scheme 1).

Proposal 1 (Scheme 2, Pathway C) is less likely in the case of mononuclear catalysts as the protonation of the $Fe^{II}-O_2$ species is likely to increase its hydrolysis rate. Proposal 2 will require a concerted electron and proton transfer to a $Fe^{III}-OOH_2$ species. A protonated $Fe^{III}-OOH_2$ species can be

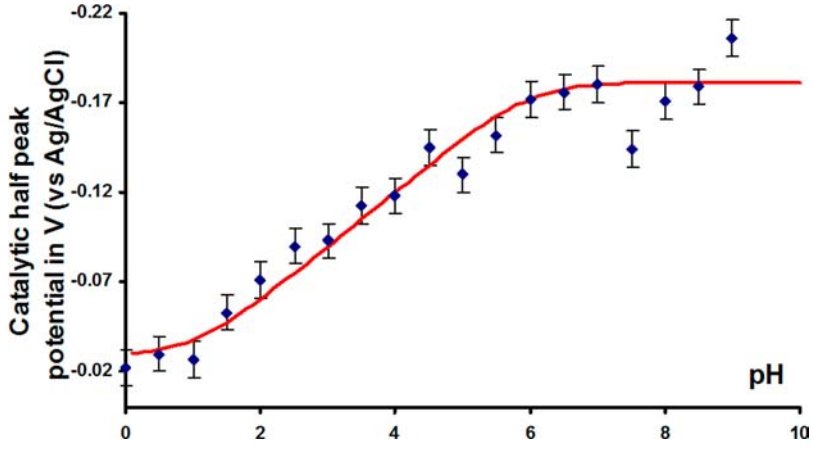

Figure 6. Plot of catalytic half peak potential vs pH.

dx.doi.org/10.1021/ic402297f | Inorg. Chem. 2013, 52, 14317–14325

Scheme 1. Possible Steps in ORR That Can Show a $2e^-/1H^+$ PCET[a]

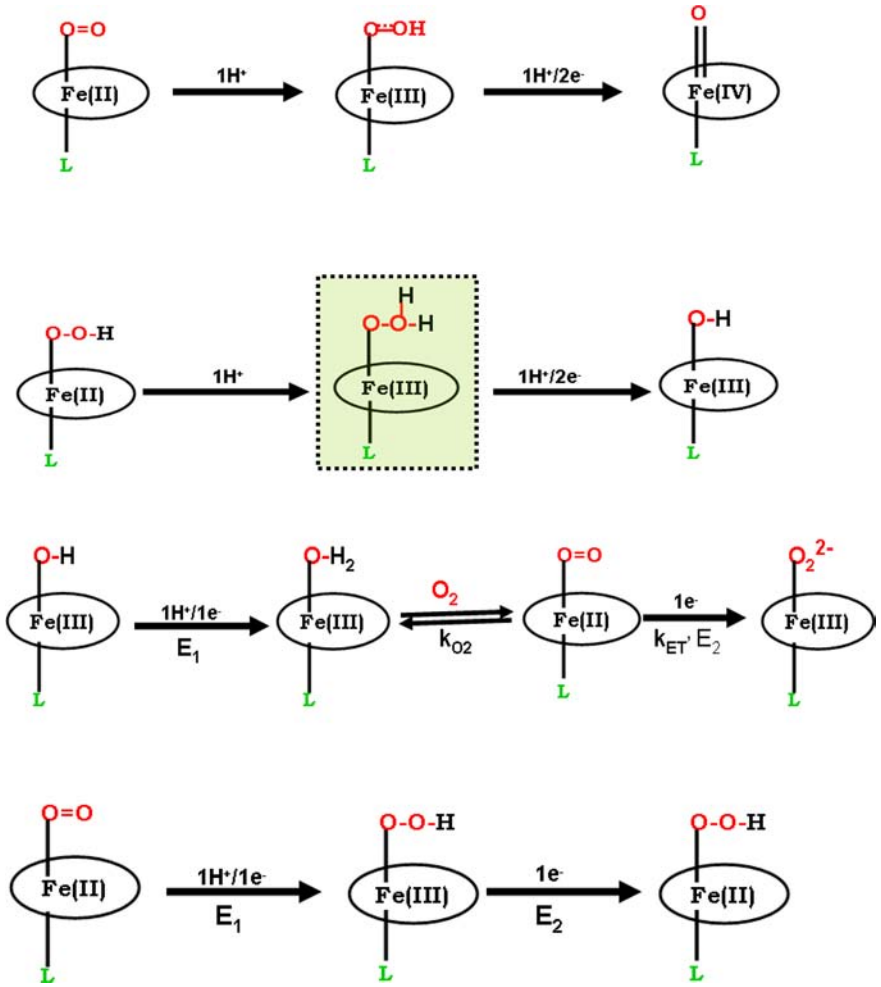

[a]From the top; **Proposal 1:** Protonation of the $Fe^{II}-O_2$ adduct followed by O−O bond cleavage involving a $2e^-/1H^+$ PCET step; **Proposal 2:** Protonation of hydroperoxo species followed by bond cleavage involving a $2e^-/1H^+$ step. The highlighted species (inside the box with brown dotted border) is expected to be unstable and undergo facile O−O bond cleavage; **Proposal 3:** Reduction of the Fe^{III} to Fe^{II} followed by oxygen binding and 1 e- transfer to the oxygenated species to generate a $Fe^{III}-O_2^{2-}$ species. For a $2e^-/1H+$ step the thermodynamic potential of the first step has to be more negative than the last, that is, $E_1 < E_2$ and $k_{O2} > k_{ET}$; **Proposal 4:** The two steps, $Fe^{II}-O_2$ to $Fe^{III}-OOH$ and reduction of $Fe^{III}-OOH$ to $Fe^{II}-OOH$, can couple to give a $2e^-/1H^+$ step provided the thermodynamic potential of the first step is more negative than the second, that is, $E_1 < E_2$.

expected to undergo facile O−O bond cleavage, hence it being the potential determining step (PDS) is slim. Proposal 3 requires simultaneous PCET reduction of a $Fe^{III}-OH$ species to $Fe^{II}-OH_2$ species, oxygen binding to result in a $Fe^{II}-O_2$ species and its reduction resulting in a $Fe^{III}-O_2^{2-}$ species. For these set of steps to show a $2e^-/H^+$ PCET the O_2 binding rate has to be much faster that the electron transfer steps and the most energy demanding step has to be reduction of the Fe^{III} species to Fe^{II} so that the subsequent reduction of a $Fe^{II}-O_2$ species to a $Fe^{III}O_2^{2-}$ is thermodynamically more feasible, that is, when the potential of the second step is higher than the first, these two steps can combine to show a $2e^-/1H^+$ PCET.[31] However, the results obtained in the organic solvent do not support this pathway. This is because the reducing agent (Na_2S) can reduce the Fe^{III} species to Fe^{II} and not the $Fe^{II}-O_2$ species (stable in the presence of excess Na_2S). This would suggest that the reduction of a $Fe^{II}-O_2$ species is thermodynamically more uphill than reduction of a Fe^{III} species. Proposal 4, to be a $2e^-/1H^+$ PCET step, will require reduction of the $Fe^{II}-O_2$ species to be thermodynamically uphill than reduction of a $Fe^{III}-OOH$ species (Scheme 2, Pathway A) such that the reduction of the $Fe^{III}-OOH$ species to a $Fe^{II}-OOH$ species will proceeds spontaneously at a potential where the $Fe^{II}-O_2$ species gets reduced to a $Fe^{III}-OOH$ species. This agrees with the observation that reduction of the $Fe^{II}-O_2$ species is indeed the most energetically demanding step in an organic medium.

The protonation required in these cases can be facilitated by the hydrogen bonding distal pocket which can also stabilize $Fe^{II}-O_2$ species. Note that the stabilization of dioxygen adduct by hydrogen bonding in this distal pocket is already demonstrated.[23] The Tafel slope of ∼120−130 mV between pH 6−9 (Supporting Information, Figure S3) suggests that the rate determining step (rds) of ORR is a one electron transfer step.[3] This could be any of the 1 e^- reduction steps depicted in Scheme 2. However most of the reduction steps in Scheme 2 have a simultaneous protonation associated with them. Since the k_{cat} is pH independent (Table 1) as well as the electron transfer to any of the $Fe^{n+}-OH_x$ ($x = 0, 1$ $n = 4, 3$) is not likely to be the r.d.s. The reduction steps are known to involve PCET

dx.doi.org/10.1021/ic402297f | Inorg. Chem. 2013, 52, 14317−14325

Scheme 2. Oxygen Reduction Mechanism in Aqueous Medium[a]

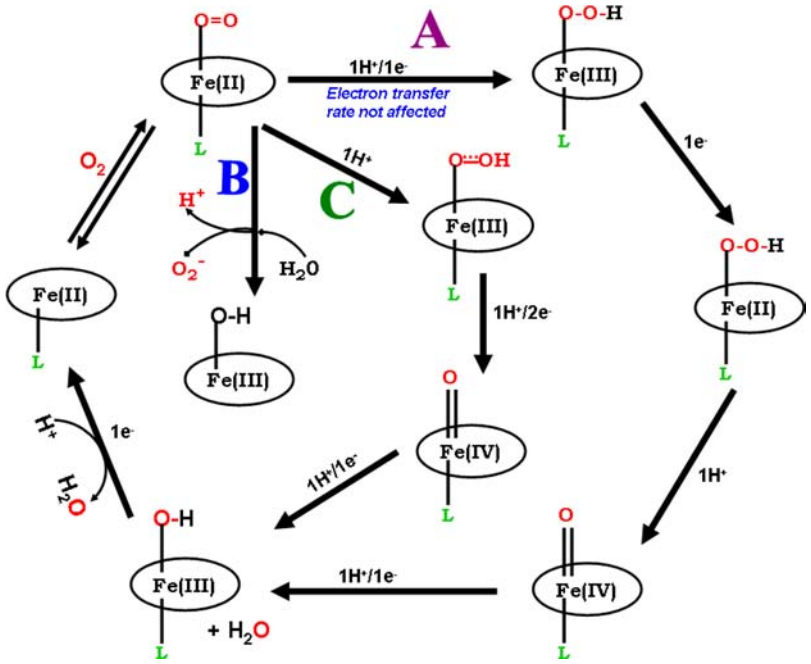

[a]In the pH range 1-9 the cycle takes **Pathway A** resulting in 4 electron reduction of O_2 to H_20. At pH = 0, when the triazoles get protonated, **Pathway B** takes its course resulting in increase in release of O_2^- which is detected as H_2O_2. **Pathway C** indicates an alternative $2e^-/1H^+$ PCET pathway involving superoxide protonation as seen in Pacman porphyrins. The abbreviation PDS stands for potential determining step in ORR electrocatalysis.

and hence should, in principle, show pH dependence. Alternatively, the reduction of Fe^{III}–OOH species to Fe^{II}–OOH, the second step of the overall $2e^-/1H^+$ PCET process, could be the r.d.s. In fact recent data on an analogous iron porphyrin (ferrocene groups replaced by ester groups) show accumulation of Fe^{III}–OOH and Fe^{IV}=O intermediates on the electrode at steady state with the help of rR spectroscopy.[34] Since the reduction of Fe^{IV}=O is likely to be a PCET step, the reduction of Fe^{III}–OOH could be the r.d.s in ORR catalyzed by these mononuclear iron porphyrin complexes.

Under neutral conditions O_2 is reduced to O_2^- in organic solvents.[20] Alternatively, in the presence of 2–3 equiv of triflic acid in organic medium and at pH > 1(in aqueous buffer), O_2 is reduced to H_2O in both mediums. When the acidity of the medium is further increased (5 equiv of triflic acid in organic medium and pH < 1 in aqueous medium), enhanced $2e^-/2H^+$ reduction is observed. Recently published results indicate that the fully reduced α_4-$FeFc_4$ catalyst binds O_2 and forms a stable Fe^{II}–O_2 adduct in an organic medium which hydrolyzes to produce O_2^-.[20] This is in spite of the presence of reducing equivalents, in the form of reduced Ferrocene groups in the distal pocket, and protic solvent (MeOH) in the medium. Only in the presence of 2–3 equiv of a strong acid does the O–O bond cleavage occur. This observation is very similar to recent reports by Fukuzumi and Karlin where rapid reduction of Cu^{II}–OOH species by ferrocene was observed in organic solvents only in the presence of acid.[27] Since the protonation of the bound O_2^- species would only lead to hydrolysis, the observe O–O bond cleavage necessitates synchronous oxidation of an electron donor species (Scheme 3).[35] Under the reaction conditions, the only available sources of this electron are the Fc residues. The resultant Fe^{III}–OOH intermediate likely undergoes fast O–O bond cleavage and may be expected to produce

Scheme 3. ORR in Organic Medium[a]

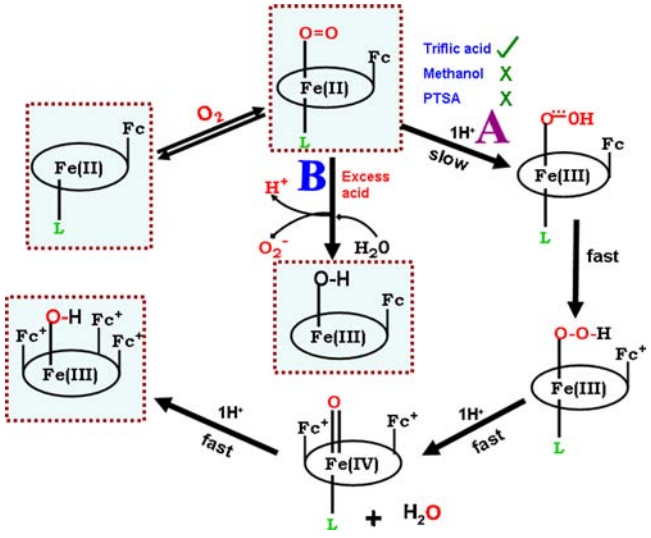

[a]On addition of 2–3 equiv of triflic acid, the cycle follows **Pathway A**. On addition of excess acid (5 equiv) the triazoles get protonated and the cycle follows **Pathway B**. Weaker acids like MeOH and PTSA can not reduce the Fe^{II}–O_2 adduct. Triflic acid being a stronger acid is required to drive the reaction forward. The species that have been identified in solution are highlighted in the (boxes with dotted brown border) scheme.

high-valent P^+·Fe^{IV}=O species. The Fe^{III}–OOH or any high-valent intermediates are not observed at −40 °C suggesting that their decay via oxidation of the other Fc groups must be fast.[27] Hence only the final hydroxide bound Fe^{III} species is observed with three Fc oxidized to Fc^+, consistent with recent proposals by Fukuzumi and Karlin.[27] Further the reduction of the Fe^{II}–

dx.doi.org/10.1021/ic402297f | Inorg. Chem. 2013, 52, 14317–14325

O_2 adduct proceeds only in the presence of a strong acid like triflic acid and not in the presence of a weak acid like PTSA. Thus in an organic medium, the $Fe^{II}-O_2$ adduct likely undergoes a proton transfer followed by electron transfer (PET) (Scheme 3, Pathway A) during ORR in presence of 2−3 equiv of acid. Three out of the four electrons required for complete reduction of oxygen to water are supplied by the ferrocenes while one is donated by iron. However the addition of excess equivalents of the acid causes the $Fe^{II}-O_2$ adduct to be hydrolyzed as superoxide which is detected as PROS (Supporting Information, Table S2). This acid catalyzed hydrolysis is very similar to the hydrolysis of the $Fe^{II}-O_2$ case when no acid is added (Scheme 3, Pathway B).

A close comparison of the results obtained in organic and aqueous medium reveals certain contrasts and analogies. Under neutral conditions O_2 is reduced to O_2^- and H_2O in organic solvents and aqueous medium, respectively. At pH > 1 and in the presence of 2−3 equiv of acid this catalyst reduced O_2 to H_2O in both aqueous and nonaqueous conditions. However when in an aqueous medium the O−O bond cleavage involves a PCET pathway; in an organic medium, where O−O cleavage does not proceed in the presence of protic solvent (MeOH) or PTSA and 2−3 equiv of triflic acid is required to drive the reaction, it likely follows a PET pathway. At pH < 1 in buffered aqueous solutions and in the presence of >5 equiv of triflic acid in organic solutions, the triazoles get protonated (pK_a = 1.5) which results in acid catalyzed hydrolysis of the iron-oxy adduct leading to enhanced production of H_2O_2 (Scheme2, Pathway B). Indeed addition of triflic acid to the resting oxidized $FeFc_4$ complex in an organic solvent produced a large change in the Soret (Supporting Information, Figure S6) but no change in the EPR data (Supporting Information, Figure S7) likely because of the protonation of the triazole group(s).

5. CONCLUSION

In summary, the α_4-$FeFc_4$ complex can act both as a homogeneous catalyst (in an organic solvent in the presence of 2−3 equiv of acid) as well as a heterogeneous catalyst (in an aqueous medium between pH 1−9) for ORR. The triazole residues, which were bound by hydrogen bonds to water molecules in the structure of the analogous Zn complex, likely provide an efficient proton transfer pathway into the active site, via hydrogen bonding, which is essential for ORR activity.[20] Further more of these residues having $pK_a \sim 1$ act as a local buffer in the vicinity of the O_2 reducing center helping the catalyst retain its selectivity for $4e^-/4H^+$ ORR over a wide range of pH. Only below pH 1 in aqueous medium or in the presence of 5 equiv of acid in organic medium, when the triazoles are likely protonated, does the selectivity of ORR decrease, and it shows enhanced H_2O_2 production due to hydrolysis of the $Fe^{II}-O_2$.

■ ASSOCIATED CONTENT

Supporting Information

Additional electrochemical data, tables of surface coverages determined from cyclic voltammetry and Tafel plots for ORR. This material is available free of charge via the Internet at http://pubs.acs.org.

■ AUTHOR INFORMATION

Corresponding Author

*E-mail: icad@iacs.res.in.

Notes

The authors declare no competing financial interest.

■ ACKNOWLEDGMENTS

This work was funded by the Department of Science and Technology, India, Grant # DST/SR/IC-35-2009 and by Council of Scientific and Industrial Research (CSIR), India, 01(2412)10/EMr-II. K.M. and S.C. acknowledge CSIR-SRF fellowship. S.S. acknowledges integrated PhD program of IACS.

■ REFERENCES

(1) Saveant, J.-M. *Chem. Rev.* **2008**, *108*, 2348.
(2) Jaouen, F.; Proietti, E.; Lefevre, M.; Chenitz, R.; Dodelet, J.-P.; Wu, G.; Chung, H. T.; Johnston, C. M.; Zelenay, P. *Energy Environ. Sci.* **2011**, *4*, 114.
(3) SongC. Z. In *PEM Fuel Cell Electrocatalysts and Catalyst Layers Fundamentals and Applications*; Zhang, J., Ed.; Springer: London, U.K., 2008.
(4) Wu, G.; Zelenay, P. *Acc. Chem. Res.* **2013**, *46*, 1878.
(5) Shin, D.; Jeong, B.; Mun, B. S.; Jeon, H.; Shin, H.-J.; Baik, J.; Lee, J. *J. Phys. Chem. C* **2013**, *117*, 11619.
(6) Liang, Y.; Wang, H.; Diao, P.; Chang, W.; Hong, G.; Li, Y.; Gong, M.; Xie, L.; Zhou, J.; Wang, J.; Regier, T. Z.; Wei, F.; Dai, H. *J. Am. Chem. Soc.* **2012**, *134*, 15849.
(7) Carver, C. T.; Matson, B. D.; Mayer, J. M. *J. Am. Chem. Soc.* **2012**, *134*, 5444.
(8) Fukuzumi, S.; Kotani, H.; Lucas, H. R.; Doi, K.; Suenobu, T.; Peterson, R. L.; Karlin, K. D. *J. Am. Chem. Soc.* **2010**, *132*, 6874.
(9) Thorseth, M. A.; Letko, C. S.; Tse, E. C. M.; Rauchfuss, T. B.; Gewirth, A. A. *Inorg. Chem.* **2013**, *52*, 628.
(10) Chang, C. J.; Loh, Z.-H.; Shi, C.; Anson, F. C.; Nocera, D. G. *J. Am. Chem. Soc.* **2004**, *126*, 10013.
(11) Kadish, K. M.; Frémond, L.; Ou, Z.; Shao, J.; Shi, C.; Anson, F. C.; Burdet, F.; Gros, C. P.; Barbe, J.-M.; Guilard, R. *J. Am. Chem. Soc.* **2005**, *127*, 5625.
(12) Ou, Z.; Lü, A.; Meng, D.; Huang, S.; Fang, Y.; Lu, G.; Kadish, K. M. *Inorg Chem.* **2012**, *51*, 8890.
(13) Schechter, A.; Stanevsky, M.; Mahammed, A.; Gross, Z. *Inorg. Chem.* **2012**, *51*, 22.
(14) Matson, B. D.; Carver, C. T.; Von Ruden, A.; Yang, J. Y.; Raugei, S.; Mayer, J. M. *Chem. Commun.* **2012**, *48*, 11100.
(15) Collman, J. P.; Boulatov, R.; Sunderland, C. J.; Fu, L. *Chem. Rev.* **2003**, *104*, 561.
(16) Forshey, P. A.; Kuwana, T. *Inorg. Chem.* **1983**, *22*, 699.
(17) Shigehara, K.; Anson, F. C. *J. Phys. Chem.* **1982**, *86*, 2776.
(18) Zhang, L.; Song, C.; Zhang, J.; Wang, H.; Wilkinson, D. P. *J. Electrochem. Soc.* **2005**, *152*, A2421.
(19) Samanta, S.; Sengupta, K.; Mittra, K.; Bandyopadhyay, S.; Dey, A. *Chem. Commun.* **2012**, *48*, 7631.
(20) Samanta, S.; Mittra, K.; Sengupta, K.; Chatterjee, S.; Dey, A. *Inorg. Chem.* **2013**, *52*, 1443.
(21) Collman, J. P.; Ghosh, S.; Dey, A.; Decréau, R. A. *Proc. Natl. Acad. Sci. U.S.A.* **2009**, *106*, 22090.
(22) Pramanik, D.; Dey, S. G. *J. Am. Chem. Soc.* **2011**, *133*, 81.
(23) Mittra, K.; Chatterjee, S.; Samanta, S.; Sengupta, K.; Bhattacharjee, H.; Dey, A. *Chem. Commun.* **2012**, *48*, 10535.
(24) Burke, J. M.; Kincaid, J. R.; Peters, S.; Gagne, R. R.; Collman, J. P.; Spiro, T. G. *J. Am. Chem. Soc.* **1978**, *100*, 6083.
(25) Wilson, S. A.; Kroll, T.; Decréau, R. A.; Hocking, R. K.; Lundberg, M.; Hedman, B.; Hodgson, K. O.; Solomon, E. I. *J. Am. Chem. Soc.* **2013**, *135*, 1124.
(26) Simultaneous oxidation of the Fc centers could not be confirmed from these data as the rR and absorption data is dominated by the porphyrin and while Fc+ is paramagnetic, it does not generally show an EPR signal at 77 K.
(27) Kakuda, S.; Peterson, R. L.; Ohkubo, K.; Karlin, K. D.; Fukuzumi, S. *J. Am. Chem. Soc.* **2013**, *135*, 6513.

(28) Mase, K.; Ohkubo, K.; Fukuzumi, S. *J. Am. Chem. Soc.* **2013**, *135*, 2800.
(29) Fukuzumi, S.; Mandal, S.; Mase, K.; Ohkubo, K.; Park, H.; Benet-Buchholz, J.; Nam, W.; Llobet, A. *J. Am. Chem. Soc.* **2012**, *134*, 9906.
(30) Bard, A. J. Faulkner, L. R. *Electrochemical Methods*; Wiley: New York, 2001.
(31) Smith, E. T.; Davis, C. A.; Barber, M. J. *Anal. Biochem.* **2003**, *323*, 114.
(32) Stine, K. J.; Andrauskas, D. M.; Khan, A. R.; Forgo, P.; D'Souza, V. T. *J. Electroanal. Chem.* **1999**, *465*, 209.
(33) Rosenthal, J.; Nocera, D. G. *Acc. Chem. Res.* **2007**, *40*, 543.
(34) Sengupta, K.; Chatterjee, S.; Samanta, S.; Dey, A. *Proc. Natl. Acad. Sci. U.S.A.* **2013**, *110*, 8431.
(35) Sengupta, K.; Chatterjee, S.; Samanta, S.; Bandyopadhyay, S.; Dey, A. *Inorg. Chem.* **2013**, *52*, 2000.